

# Soft physics and exclusive Higgs production at the LHC<sup>1</sup>

A.D. Martin<sup>a</sup>, M.G. Ryskin<sup>a,b</sup> and V.A. Khoze<sup>a,b</sup>

<sup>a</sup> Institute for Particle Physics Phenomenology, University of Durham, Durham, DH1 3LE

<sup>b</sup> Petersburg Nuclear Physics Institute, Gatchina, St. Petersburg, 188300, Russia

## Abstract

We discuss two inter-related topics: a multi-component  $s$ - and  $t$ -channel model of ‘soft’ high-energy  $pp$  interactions and the properties of the exclusive Higgs signal at the LHC.

## 1 Introduction

We begin by drawing attention to the exciting possibility of studying the Higgs sector via the exclusive process  $pp \rightarrow p + H + p$  at the LHC, where the  $+$  signs denote the presence of large rapidity gaps. The prediction of the event rate of such a process depends on an interesting mixture of ‘soft’ and ‘hard’ physics. We explain why the former requires the development of a multi-component  $s$ - and  $t$ -channel model of high-energy ‘soft’ processes, in which absorptive effects play a key role. We describe how the model may be used to estimate the survival probability of the large rapidity gaps to eikonal and enhanced soft rescattering. We comment on other models used to calculate the survival factors.

We note that CDF experiments at the Tevatron have already measured the rate of similar exclusive processes, namely  $pp \rightarrow p + A + p$  where  $A = \gamma\gamma$  or dijet or  $\chi_c$  [1]. These processes are driven by the same theoretical mechanism used to estimate the exclusive Higgs signal. The agreement of the CDF experimental rates with the model predictions leads to optimism of the use of very forward proton taggers to explore the Higgs sector at the LHC [2].

The discussion here is brief, with a minimum of references. More details, and references, can be found in two recent reviews covering the same material [3, 4].

## 2 Advantages of the exclusive Higgs signal with $H \rightarrow b\bar{b}$

The exclusive process  $pp \rightarrow p + H + p$  for the production of a Higgs at the LHC with mass  $M_H \lesssim 140$  GeV, where the dominant decay mode is  $H \rightarrow b\bar{b}$ , has the following advantages:

- The mass of the Higgs boson (and in some cases the width) can be measured with high accuracy (with mass resolution  $\sigma(M) \sim 1$  GeV) by measuring the missing mass to the forward outgoing protons, *provided* that they can be accurately tagged some 400 m from the interaction point.

---

<sup>1</sup>Based on a talk by Alan Martin at the UCL Workshop on “Standard Model discoveries with early LHC data”, 30 March - 1 April, 2009

- It offers a unique chance to study  $H \rightarrow b\bar{b}$ , since the leading order  $b\bar{b}$  QCD background is suppressed by the  $P$ -even  $J_z = 0$  selection rule, where the  $z$  axis is along the direction of the proton beam. Indeed, at LO, this background vanishes in the limit of massless  $b$  quarks and forward outgoing protons. Moreover, a measurement of the mass of the decay products must match the ‘missing mass’ measurement. For a SM Higgs the signal-to-background ratio  $S/B \sim O(1)$
- The quantum numbers of the central object (in particular, the  $C$ - and  $P$ -parities) can be analysed by studying the azimuthal angle distribution of the tagged protons. Due to the selection rules, the production of  $0^{++}$  states is strongly favoured.
- There is a clean environment for the exclusive process — this is even possible with overlapping interactions (pile-up) using fast timing detectors with very good resolution: 10 ps or better.
- For SUSY Higgs there are regions of SUSY parameter space where the signal is enhanced by a factor of 10 or more, while the background remains unaltered. Moreover, there are domains of parameter space where Higgs boson production via the conventional inclusive processes is suppressed whereas the exclusive signal is enhanced, and even such, that both the  $h$  and  $H$   $0^{++}$  bosons may be detected.

### 3 Is the exclusive Higgs cross section large enough?

What is the price that we pay for the large rapidity gaps? How do we calculate the cross section for the exclusive process  $pp \rightarrow p + H + p$ ? The calculation of the exclusive production of a heavy system is an interesting mixture of *soft* and *hard* QCD effects. The basic mechanism is shown in Fig. 1. The  $t$ -integrated cross section is of the form

$$\sigma \simeq \frac{S^2}{B^2} \left| N \int \frac{dQ_t^2}{Q_t^4} f_g(x_1, x'_1, Q_t^2, \mu^2) f_g(x_2, x'_2, Q_t^2, \mu^2) \right|^2, \quad (1)$$

where  $B/2$  is the  $t$ -slope of the proton-Pomeron vertex, and  $N$  is given in terms of the  $H \rightarrow gg$  decay width. The probability amplitudes,  $f_g$ , to find the appropriate pairs of  $t$ -channel gluons  $(x_1, x'_1)$  and  $(x_2, x'_2)$ , are given by the skewed unintegrated gluon densities at a hard scale  $\mu \sim M_H/2$ . Since  $(x' \sim Q_t/\sqrt{s}) \ll (x \sim M_H/\sqrt{s}) \ll 1$ , it is possible to express  $f_g(x, x', Q_t^2, \mu^2)$ , to single log accuracy, in terms of the conventional integrated density  $g(x)$ , together with a known Sudakov suppression factor  $T$ , which ensures that the active gluons do not radiate in the evolution from  $Q_t$  up to the hard scale  $\mu \sim M_H/2$ , and so preserves the rapidity gaps. The factor  $T$  ensures that the integral is infrared stable, and may be calculated by perturbative QCD.

If we were to neglect the rapidity gaps survival factor,  $S^2$  in (1), then QCD predicts that the exclusive cross for producing a SM Higgs of mass 120 GeV would be more than 100 fb at an LHC energy of  $\sqrt{s} = 14$  TeV.

The factor  $S^2$  in (1) is the probability that the secondaries, which are produced by soft rescattering, do not populate the rapidity gaps. As written, the cross section assumes soft-hard

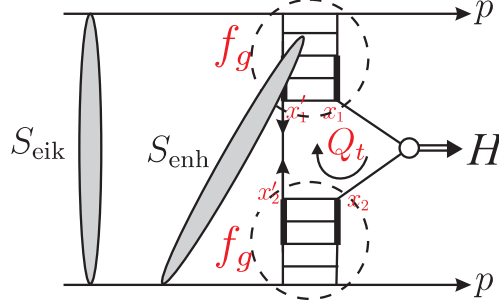


Figure 1: The mechanism for the exclusive process  $pp \rightarrow p + H + p$ , with the eikonal and enhanced survival factors shown symbolically. The thick lines on the Pomeron ladders, either side of the subprocess ( $gg \rightarrow H$ ), indicate the rapidity interval  $\Delta y$  where enhanced absorption is not permitted, see Section 7.3.

factorization. In other words, the survival factor, denoted by  $S_{\text{eik}}$  in Fig. 1, and calculated from an eikonal model of soft interactions, does not depend on the structure of the perturbative QCD amplitude embraced by the modulus signs in (1). Actually the situation is more complicated. There is the possibility of enhanced rescattering which involves intermediate partons, and which breaks soft-hard factorization. To calculate the corresponding survival factors,  $S_{\text{eik}}$  and  $S_{\text{enh}}$ , we need, first, a model for soft high-energy  $pp$  interactions. We come back to the estimation of  $\sigma(pp \rightarrow p + H + p)$  in Section 7.3.

## 4 Requirements of a model of soft interactions

Besides the need for calculating the rapidity gap survival factors, it is valuable to revisit the ‘soft’ domain at this time because of the intrinsic interest in obtaining a reliable self-consistent model of high-energy soft interactions which may soon be illuminated by data from the LHC. Moreover, we need a reliable model so as to be able to predict the gross features of soft interactions; in particular to understand the structure of the underlying events at the LHC.

What are the requirements of such a high-energy model? It should be self-consistent theoretically – it should satisfy unitarity; absorptive corrections are large and imply the importance of multi-Pomeron contributions. The model should describe all the available soft data in the CERN-ISR to Tevatron energy range. Finally, the model should include Pomeron components of different size so that we can allow for the effects of soft-hard factorization breaking.


The total and elastic proton-proton cross sections are usually described in terms of an eikonal model, which automatically satisfies  $s$ -channel elastic unitarity. The unitarity relation is diagonal in impact parameter  $b$ , and so these reactions can be described in terms of the opacity  $\Omega(s, b) \geq 0$

$$d\sigma_{\text{tot}}/d^2b = 2(1 - e^{-\Omega/2}), \quad d\sigma_{\text{el}}/d^2b = (1 - e^{-\Omega/2})^2, \quad (2)$$

see Fig. 2(a). The Good-Walker formalism [5] is used to account for the possibility of excitation of the initial proton, that is for two-particle intermediate states with the proton replaced by  $N^*$

(a) Elastic amplitude

$$\text{Im} A_{\text{el}} = \overline{\text{Diagram}} = 1 - e^{-\Omega/2} = \sum_{n=1}^{\infty} \overline{\text{Diagram}} \Omega/2$$

(b) Inclusion of low-mass dissociation 

$$\text{Im} A_{ik} = \overline{\text{Diagram}}^i_k = 1 - e^{-\Omega_{ik}/2} = \sum \overline{\text{Diagram}} \Omega_{ik}/2$$

(c) Inclusion of high-mass dissociation

$$\Omega_{ik} = \overline{\text{Diagram}}^i_k + \overline{\text{Diagram}}^i_k \}_M + \overline{\text{Diagram}} + \dots \overline{\text{Diagram}} + \dots$$

Figure 2: (a) The single-channel eikonal description of elastic scattering; (b) the multichannel eikonal formula which allows for low-mass proton dissociations in terms of diffractive eigenstates  $|\phi_i\rangle$ ,  $|\phi_k\rangle$ ; and (c) the inclusion of the multi-Pomeron-Pomeron diagrams which allow for high-mass dissociation.

resonances, Fig. 2(b). Diffractive eigenstates  $|\phi_i\rangle$  are introduced which only undergo ‘elastic’ scattering. That is, we go from a single elastic channel to a multi-channel eikonal,  $\Omega_{ik}$ . Already at Tevatron energies the absorptive correction to the elastic amplitude, due to elastic eikonal rescattering, gives about a 20% reduction of simple one-Pomeron exchange. After accounting for low-mass proton excitations, the correction becomes twice larger (that is, up to a 40% reduction).

At first sight, by enlarging the number of eigenstates  $|\phi_i\rangle$  it seems we may even allow for high-mass proton dissociation. However, here, we face the problem of double counting when the partons originating from dissociation of the beam and ‘target’ initial protons overlap in rapidities. For this reason, high-mass ( $M$ ) dissociation is usually described by “enhanced” multi-Pomeron diagrams. The first, and simplest, such contribution to single proton dissociation  $d\sigma_{\text{SD}}/dM^2$ , is the triple-Pomeron graph, see Fig. 2(c). The absorptive effects in the triple-Regge domain are expected to be quite large ( $\lesssim 80\%$ ), since there is an extra factor of 2 from the AGK cutting rules [6]. Recent triple-Regge analyses [7], which include screening effects, of the available data find that the *bare* triple-Pomeron coupling is indeed much larger than the (effective) value found in the original (unscreened) analyses. This can be anticipated by simply noting that since the original triple-Regge analyses did not include absorptive corrections, the resulting triple-Regge couplings must be regarded, not as bare vertices, but as effective couplings embodying the absorptive effects. That is,

$$g_{3P}^{\text{effective}} \simeq S^2 g_{3P}^{\text{bare}}, \quad (3)$$

where  $S^2$  is the survival probability of the rapidity gap. Due to the large bare triple-Pomeron

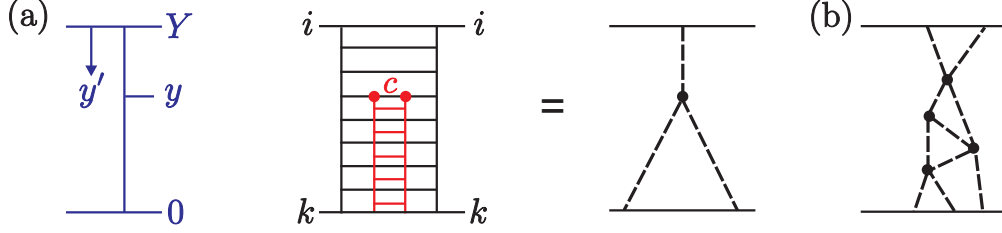


Figure 3: (a) The ladder structure of the triple-Pomeron amplitude between diffractive eigenstates  $|\phi_i\rangle, |\phi_k\rangle$  of the proton; the rapidity  $y$  spans an interval 0 to  $Y = \ln s$ . (b) A multi-Pomeron diagram.

coupling ( $g_{3P} = \lambda g_N$  with  $\lambda \simeq 0.25$ , where  $g_N$  is the Pomeron-proton coupling), we need a model of soft high-energy processes which includes multi-Pomeron interactions, see, for example, the final diagrams in Fig. 2(c).

## 5 Multi-component $s$ - and $t$ -channel model

Here we follow a *partonic* approach to obtain a model high-energy soft interactions [8]. While the eikonal formalism describes the rescattering of the incoming fast particles, the enhanced multi-Pomeron diagrams represent the rescattering of the intermediate partons in the ladder (Feynman diagram) which describes the Pomeron-exchange amplitude. We refer to Fig. 3. The multi-Pomeron effects are included by the following equation describing the evolution in rapidity  $y$  of the opacity  $\Omega_k$  starting from the ‘target’ diffractive eigenstate  $|\phi_k\rangle$ :

$$\frac{d\Omega_k(y, b)}{dy} = e^{-\lambda\Omega_i(y', b)/2} e^{-\lambda\Omega_k(y, b)/2} \left( \Delta + \alpha' \frac{d^2}{d^2b} \right) \Omega_k(y, b), \quad (4)$$

where  $y' = \ln s - y$ . Let us explain the meanings of the three factors on the right-hand-side of (4). If only the last factor,  $(\dots)\Omega_k$ , is present then the evolution generates the ladder-type structure of the bare Pomeron exchange amplitude, where the Pomeron trajectory  $\alpha_P = 1 + \Delta + \alpha't$ . The inclusion of the preceding factor allows for rescatterings of an intermediate parton  $c$  with the “target” proton  $k$ ; Fig. 3(a) shows the simplest (single) rescattering which generates the triple-Pomeron diagram. Finally, the first factor allows for rescatterings with the beam  $i$ . In this way the absorptive effects generated by all multi-Pomeron diagrams are included, like the one shown in Fig. 3(b). There is an analogous equation for the evolution in rapidity  $y'$  of  $\Omega_i(y', b)$  starting from the ‘beam’ diffractive eigenstate  $|\phi_i\rangle$ . The two equations may be solved iteratively.

As we are dealing with elastic *amplitudes* we use  $e^{-\lambda\Omega/2}$  and not  $e^{-\lambda\Omega}$ . The coefficient  $\lambda$  in the exponents arises since parton  $c$  will have a different absorption cross section from that of the diffractive eigenstates. Naively, we may assume that the states  $i, k$  contains a number  $1/\lambda$  of partons. The factors  $e^{-\lambda\Omega/2}$  generate multi-Pomeron vertices of the form

$$g_m^n = n m \lambda^{n+m-2} g_N / 2 \quad \text{for } n + m \geq 3, \quad (5)$$

where a factor  $1/n!$ , which comes from the expansion of the exponent, accounts for the identity of the Pomerons. The factors  $n(m)$  allow for the  $n(m)$  possibilities to select the Pomeron  $\Omega_i(\Omega_k)$  which enters the evolution (4) from the  $n(m)$  identical Pomerons. In principle, the vertices  $g_m^n$  are unknown. However, the above ansatz is physically motivated and is certainly better than to assume only a triple-Pomeron coupling, that is, to assume that  $g_m^n = 0$  for  $n + m > 3$ .

Even though  $\lambda \simeq 0.2 - 0.25$ , the role of factors  $e^{-\lambda\Omega/2}$  is not negligible, since the suppression effect is accumulated throughout the evolution. For instance, if  $\lambda \ll 1$  the full absorptive correction is given by the product  $\lambda\Omega Y/2$ , where the small value of  $\lambda$  is compensated by the large rapidity interval  $Y$ .

So far, we have allowed multi-components in the  $s$ -channel via a multichannel eikonal. However, a novel feature of the model of Ref. [8] is that four different  $t$ -channel states are included. One for the secondary Reggeon ( $R$ ) trajectory, and three Pomeron states ( $P_1, P_2, P_3$ ) to mimic the BFKL diffusion in the logarithm of parton transverse momentum,  $\ln(k_t)$ . Recall that the BFKL Pomeron is not a pole in the complex  $j$ -plane, but a branch cut. Here the cut is approximated by three  $t$ -channel states of a different size. The typical values of  $k_t$  are  $k_{t1} \sim 0.5$  GeV,  $k_{t2} \sim 1.5$  GeV and  $k_{t3} \sim 5$  GeV for the large-, intermediate- and small-size components of the Pomeron, respectively. Thus (4) is rewritten as a four-dimensional matrix equation for  $\Omega_k^a$  in  $t$ -channel space ( $a = P_1, P_2, P_3, R$ ), as well as being a three-channel eikonal in diffractive eigenstate  $|\phi_k\rangle$  space. The transition terms, added to the equations, which couple the different  $t$ -channel components, are fixed by the properties of the BFKL equation. So, in principle, we have the possibility to explore the matching of the soft Pomeron (approximated by the large-size component  $P_1$ ) to the QCD Pomeron (approximated by the small-size component  $P_3$ ). The key parameters which drive the evolution in rapidity are the intercepts  $1 + \Delta^a$  and the slopes  $\alpha'_a$  of the  $t$ -channel exchanges.

The model is tuned to describe all the available soft data in the CERN-ISR to Tevatron energy range. In principle, it may be used to predict all features of soft interactions at the LHC. All components of the Pomeron are taken to have a *bare* intercept  $\Delta \equiv \alpha_P(0) - 1 = 0.3$ , consistent with resummed NLL BFKL. However, the large-size Pomeron component is heavily screened by the effect of ‘enhanced’ multi-Pomeron diagrams, that is, by high-mass dissociation, which results in  $\Delta_{\text{eff}} \sim 0.08$  and  $\alpha'_{\text{eff}} \sim 0.25$ . This leads, among other things, to the saturation of the particle multiplicity at low  $p_t$ , and to a slow growth of the total cross section. Indeed, the model predicts a relatively low total cross section at the LHC –  $\sigma_{\text{tot}}(\text{LHC}) \simeq 90$  mb. On the other hand, the small-size component of the Pomeron is weakly screened, leading to an anticipated growth of the particle multiplicity at large  $p_t$  ( $\sim 5$  GeV) at the LHC. Thus the model has the possibility to embody a smooth matching of the perturbative QCD Pomeron to the ‘soft’ Pomeron.

## 6 Long-range rapidity correlations

We emphasize that each multi-Pomeron exchange diagram describes simultaneously a few different processes. The famous AGK cutting rules [6] gives the relation between the different subprocesses originating from the same diagram.

Note that the eikonal model predicts a long-range correlation between the secondaries produced in different rapidity intervals. Indeed, we have possibility to cut any number of Pomerons. Cutting  $n$  Pomerons we get an event with multiplicity  $n$  times larger than that generated by one Pomeron. The probability to observe a particle from a diagram where  $n$  Pomerons are cut is  $n$  times larger than that from the diagram with only one cut Pomeron. The observation of a particle at rapidity  $y_a$ , say, has the effect of enlarging the relative contribution of diagrams with a larger number of cut Pomerons. For this reason the probability to observe another particle at quite a different rapidity  $y_b$  becomes larger as well. This can be observed experimentally via the ratio of inclusive cross sections

$$R_2 = \frac{\sigma_{\text{inel}} d^2\sigma/dy_a dy_b}{(d\sigma/dy_a)(d\sigma/dy_b)} - 1 = \frac{d^2N/dy_a dy_b}{(dN/dy_a)(dN/dy_b)} - 1, \quad (6)$$

where  $dN/dy = (1/\sigma_{\text{inel}})d\sigma/dy$  is the particle density.

Without multi-Pomeron effects the value of  $R_2$  exceeds zero only when the two particles are close to each other, that is when the separation  $|y_a - y_b| \sim 1$  is not large. Such short-range correlations arise from resonance or jet production. However, multi-Pomeron exchange leads to a long-range correlation,  $R_2 > 0$ , even for a large rapidity difference between the particles,  $|y_a - y_b| \sim Y$ .

## 7 Rapidity gap survival

Now that we have a model of high-energy soft interactions, we can estimate the rapidity gap survival factors  $S_{\text{eik}}^2$  and  $S_{\text{enh}}^2$  of the process  $pp \rightarrow p + H + p$  shown in Fig. 1. We start with  $S_{\text{eik}}^2$ .

### 7.1 Eikonal rescattering

The gap survival factor caused by *eikonal* rescattering of the diffractive eigenstates [5], for a fixed impact parameter  $\mathbf{b}$ , is

$$S_{\text{eik}}^2(\mathbf{b}) = \frac{\left| \sum_{i,k} |a_i|^2 |a_k|^2 \mathcal{M}_{ik}(\mathbf{b}) \exp(-\Omega_{ik}^{\text{tot}}(s, \mathbf{b})/2) \right|^2}{\left| \sum_{i,k} |a_i|^2 |a_k|^2 \mathcal{M}_{ik}(\mathbf{b}) \right|^2}. \quad (7)$$

where  $\Omega_{ik}^{\text{tot}}(s, \mathbf{b})$  is the total opacity of the  $ik$  interaction, and the  $a_i$ 's occur in the decomposition of the proton wave function in terms of diffractive eigenstates  $|p\rangle = \sum_i a_i |\phi_i\rangle$ . The total opacity has the form  $\Omega_k^a(y)\Omega_i^a(y')$  integrated over the impact parameters  $\mathbf{b}_1, \mathbf{b}_2$  (keeping a fixed impact parameter separation  $\mathbf{b} = \mathbf{b}_1 - \mathbf{b}_2$  between the incoming protons) and summed over the different Pomeron components  $a$ . Recall  $y' = Y - y = \ln s - y$ , see Fig. 3. The exact shape of the matrix element  $\mathcal{M}_{ik}$  for the hard subprocess  $gg \rightarrow H$  in  $\mathbf{b}$  space and the relative couplings to the various diffractive eigenstates  $i, k$  should be addressed further.

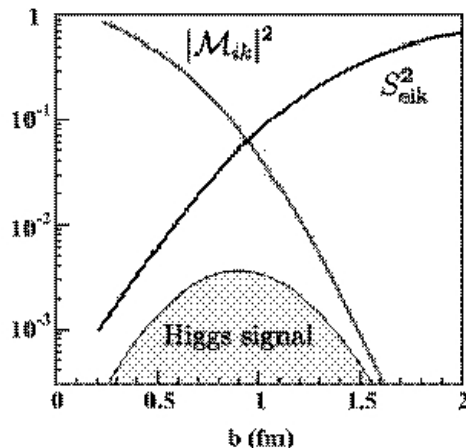


Figure 4: A “first look” at the impact parameter dependence of the signal for 120 GeV Higgs production at the LHC after including an eikonal rescattering correction.

One possibility is to say that the  $\mathbf{b}$  dependence of  $\mathcal{M}$  should be, more or less, the same as that observed for diffractive  $J/\psi$  electroproduction ( $\gamma + p \rightarrow J/\psi + p$ ), and the coupling to the  $|\phi_i\rangle$  component of the proton should be proportional to the same factor  $\gamma_i$  as in a soft interaction. This leads to

$$\mathcal{M}_{ik} \propto \gamma_i \gamma_k \exp(-b^2/4B) \quad (8)$$

with  $t$ -slope  $B \simeq 4 \text{ GeV}^{-2}$ . The resulting “first look” predictions obtained using the ‘soft’ model of [8], for the exclusive production of a scalar 120 GeV Higgs at the LHC, are shown in Fig. 4. After we integrate over  $b$ , we find that the survival probability of the rapidity gaps in  $pp \rightarrow p + H + p$  to eikonal rescattering is  $\langle S_{\text{eik}}^2 \rangle = 0.017$ , with the Higgs signal concentrated around impact parameter  $b = 0.8 \text{ fm}$ . Expressing the survival factors in this manner is too simplistic and even sometimes misleading, for the reasons we shall explain below; nevertheless these numbers are frequently used as a reference point.

## 7.2 Enhanced rescattering

As indicated in Fig. 1, besides *eikonal* screening,  $S_{\text{eik}}$ , caused by soft interactions between the protons, we must also consider so-called ‘*enhanced*’ rescattering,  $S_{\text{enh}}$ , which involves intermediate partons. Since we have to multiply the probabilities of absorption on each individual intermediate parton, the final effect is *enhanced* by the large multiplicity of intermediate partons. Unlike  $S_{\text{eik}}^2(\mathbf{b})$ , the enhanced survival factor  $S_{\text{enh}}^2(\mathbf{b})$  cannot be considered simply as an overall multiplicative factor. The probability of interaction with a given intermediate parton depends on its position in configuration space; that is, on its impact parameter  $\mathbf{b}$  and its momentum  $k_t$ . This means that  $S_{\text{enh}}$  simultaneously changes the distribution of the active partons which finally participate in the hard subprocess. It breaks the soft-hard factorization of (1).

Do we anticipate that  $S_{\text{enh}}$  will be important? Working at LO (of the collinear approximation) we would expect that effect may be neglected. Due to strong  $k_t$ -ordering the transverse



momenta of all the intermediate partons are very large (i.e. the transverse size of the Pomeron is very small) and therefore the absorptive effects are negligible. Nevertheless, this may be not true at a very low  $x$ , say  $x \sim 10^{-6}$ , where the parton densities become close to saturation and the small value of the absorptive cross section is compensated by the large value of the parton density. Indeed, the contribution of the first *enhanced* diagram, which describes the absorption of an intermediate parton, was estimated in the framework of the perturbative QCD in Ref.[9]. It turns out that it could be quite large. On the other hand, such an effect does not reveal itself experimentally. The absorptive corrections due to enhanced screening must increase with energy. This is not observed in the present data (see [10] for a more detailed discussion). One reason is that the gap survival factor  $S_{\text{eik}}^2$  already absorbs almost the whole contribution from the centre of the disk. The parton essentially only survives eikonal rescattering on the periphery; that is, at large impact parameters  $b$ . On the other hand, on the periphery, the parton density is rather small and the probability of *enhanced* absorption is not large.

### 7.3 Gap survival for exclusive Higgs production

Now, the model of Ref. [8], with its multi-component Pomeron, allows us to calculate the survival probability of the rapidity gaps, to *both* eikonal and enhanced rescattering. Recall that the evolution equations in rapidity (like (4)) have a matrix form in  $aa'$  space, where  $a = 1, 2, 3$  correspond to the large-, intermediate- and small-size components of the Pomeron. We start the evolution from the large component  $P_1$ , and since the evolution equations allow for a transition from one component to another (corresponding to BFKL diffusion in  $\ln k_t$  space), we determine how the enhanced absorption will affect the high- $k_t$  distribution in the small-size component  $P_3$ , which contains the active gluon involved in forming the Higgs. Moreover, at each step of the evolution the equations include absorptive factors of the form  $e^{-\lambda(\Omega_k^a + \Omega_i^a)/2}$ . By solving the equations with and without these suppression factors, we could quantify the effect of enhanced absorption. However, there are some subtle issues here. First, since we no longer have soft-hard factorization, we must first specify exactly what is included in the bare hard amplitude.

Another relevant observation is that the phenomenologically determined generalised gluon distributions are usually taken at  $p_t = 0$ , and then the observed “total” cross section is calculated by integrating over  $p_t$  of the recoil protons *assuming* an exponential behaviour  $e^{-Bp_t^2}$ ; that is

$$\sigma = \int \frac{d\sigma}{dp_{1t}^2 dp_{2t}^2} dp_{1t}^2 dp_{2t}^2 = \frac{1}{B^2} \left. \frac{d\sigma}{dp_{1t}^2 dp_{2t}^2} \right|_{p_{1t}=p_{2t}=0}, \quad (9)$$

where

$$\int dp_t^2 e^{-Bp_t^2} = 1/B = \langle p_t^2 \rangle. \quad (10)$$

However, the total soft absorptive effect changes the  $p_t$  distribution in comparison to that for the bare cross section determined from perturbative QCD. Moreover, the correct  $p_t$  dependence of the matrix element  $\mathcal{M}$  of the hard  $gg \rightarrow H$  subprocess does *not* have an exponential form. Thus the additional factor introduced by the soft interactions is not just the gap survival  $S^2$ , but rather  $S^2 \langle p_t^2 \rangle^2$ , where the square arises since we have to integrate over the  $p_t$  distributions of *two* outgoing protons. Indeed in all the previous calculations the soft prefactor had the form

$S^2/B^2$ . Note that, using the model of Ref. [8], we no longer have to *assume* an exponential  $\mathbf{b}$  behaviour of the matrix element. Now the  $\mathbf{b}$  dependence of  $\mathcal{M}(\mathbf{b})$  is driven by the opacities, and so is known. Thus we present the final result in the form  $S^2\langle p_t^2 \rangle^2$ . That is, we replace  $S^2/B^2$  in (1) by  $S^2\langle p_t^2 \rangle^2$ . So if we wish to compare the improved treatment with previous predictions obtained assuming  $B = 4 \text{ GeV}^{-2}$  we need to introduce the “renormalisation” factor  $(\langle p_t^2 \rangle B)^2$ . The resulting (effective) value is denoted by  $S_{\text{eff}}^2$ .

Before we do this, there is yet another effect that we must include. We have to allow for a threshold in rapidity [10]. The evolution equation for  $\Omega_k^a$ , (4), and the analogous one for  $\Omega_i^a$ , are written in the leading  $\ln(1/x)$  approximation, without any rapidity threshold. The emitted parton, and correspondingly the next rescattering, is allowed to occur just after the previous step. On the other hand, it is known that a pure kinematical  $t_{\text{min}}$  effect suppresses the probability to produce two partons close to each other. Moreover, this  $t_{\text{min}}$  effect becomes especially important near the production vertex of the heavy object. It is, therefore, reasonable to introduce some threshold rapidity gap,  $\Delta y$ , and to compute  $S_{\text{enh}}^2$  only allowing for absorption outside this threshold interval, as indicated in Fig. 1. For exclusive Higgs boson production at the LHC, the model gives  $S_{\text{eff}}^2 = 0.004, 0.009$  and  $0.015$  for  $\Delta y = 0, 1.5$  and  $2.3$  respectively [11]. For  $\Delta y = 2.3$  all the NLL BFKL corrections may be reproduced by the threshold effect.

Furthermore, Ref. [11] presents arguments that

$$\langle S_{\text{eff}}^2 \rangle = 0.015^{+0.01}_{-0.005} \quad (11)$$

should be regarded as a *conservative* (lower) limit for the gap survival probability in the exclusive production of a SM Higgs boson of mass 120 GeV at the LHC energy of  $\sqrt{s} = 14 \text{ TeV}$ . Recall that this effective value should be compared with  $S^2$  obtained using the exponential slope  $B = 4 \text{ GeV}^{-2}$ . The resulting value for the cross section is, conservatively,

$$\sigma(pp \rightarrow p + H + p) \simeq 2 - 3 \text{ fb}, \quad (12)$$

with an uncertainty<sup>2</sup> of a factor of 3 up or down.

## 7.4 Comments on other estimates of $S^2$

A very small value  $S_{\text{enh}}^2 = 0.063$  is claimed in [12], which would translate into an *extremely* small value of  $S_{\text{eff}}^2 = 0.0235 \times 0.063 = 0.0015$ . There are many reasons why this estimate is invalid. In this model the two-particle irreducible amplitude depends on the impact parameter  $b$  *only* through the form factors of the incoming protons. The enhanced absorptive effects (which result from the sum of the enhanced diagrams) are the same at any value of  $b$ . Therefore, the enhanced screening effect does not depend on the initial parton density at a particular impact parameter  $b$ , and does not account for the fact that at the periphery of the proton, from where the main contribution comes (after the  $S_{\text{eik}}$  suppression), the parton density is much smaller than that in the centre. For this reason the claimed value of  $S_{\text{enh}}^2$  is much too small. Besides

---

<sup>2</sup>Besides the uncertainty arising from that on  $S_{\text{eff}}^2$ , the other main contribution to the error comes from that on the unintegrated gluon distributions,  $f_g$ , which enter to the fourth power.

this lack of  $k_t \leftrightarrow b$  correlation, the model has no diagrams with odd powers of  $g_{3P}$ . For example, the lowest triple-Pomeron diagram is *missing*. That is, the approach does not contain the first, and most important at the lower energies, absorptive correction. Next, recall that in a theory which contains the triple-Pomeron coupling only, without the four-Pomeron term (and/or more complicated multi-Pomeron vertices), the total cross section *decreases* at high energies. On the other hand, the approximation used in [12] leads to saturation (that is, to a constant cross section) at very high energies. In other words, the approach is not valid at high energies<sup>3</sup>. This means that such an approximation can only be justified in a limited energy interval; at very high energies it is inconsistent with asymptotics, while at relatively low energies the first term, proportional to the first power of the triple-Pomeron coupling  $g_{3P}$ , is missing. Finally, the predictions of the model of [12] have not been compared to the CDF exclusive data of Section 8.

The values of  $x \sim 10^{-6}$  relevant to the evaluation of  $S_{\text{enh}}^2$  at LHC energies are quite small. At leading order (LO) the gluon density increases with  $1/x$ . So, at first sight, it appears that this may lead to the Black Disk Regime where the enhanced absorptive corrections will cause the cross section for exclusive production to practically vanish. This is the basis of the low value of  $S_{\text{enh}}^2$  estimated in [13]. However, NLO global parton analyses show that at relatively low scales ( $k_t^2 = \mu^2 \sim 2 - 4 \text{ GeV}^2$ ) the gluons are flat for  $x < 10^{-3} - 10^{-4}$  (or even decrease when  $x \rightarrow 0$ ). Recall that the contribution of enhanced diagrams from larger scales decrease as  $1/k_t^2$  (see [9]). The anomalous dimension  $\gamma < 1/2$  is not large and so the growth of the gluon density,  $xg(x, \mu^2) \propto (\mu^2)^\gamma$ , cannot compensate the factor  $1/k_t^2$ . Therefore the whole enhanced diagram contribution should be evaluated at rather low scales where the NLO gluon is flat<sup>4</sup> in  $x$ . Thus there is no reason to expect a strong energy dependence of  $S_{\text{enh}}^2$ .

Another observation against the extremely small gap survival factor,  $S_{\text{enh}}$ , estimated in [12, 13] is that the analysis of [11] shows the following hierarchy of the size of the gap survival factor to enhanced rescattering

$$S_{\text{enh}}^{\text{LHC}}(M_H > 120 \text{ GeV}) > S_{\text{enh}}^{\text{Tevatron}}(\gamma\gamma; E_T > 5 \text{ GeV}) > S_{\text{enh}}^{\text{Tevatron}}(\chi_c), \quad (13)$$

which reflects the size of the various rapidity gaps of the different exclusive processes. The fact that  $\gamma\gamma$  and  $\chi_c$  events have been observed at the Tevatron confirms that there is no danger that enhanced absorption will strongly reduce the exclusive SM Higgs signal at the LHC energy.

## 8 Exclusive processes at the Tevatron and the LHC

In preparation for the studies of the exclusive process,  $pp \rightarrow p+H+p$ , at the LHC, it is important to know how reliable is the ‘Durham’ prediction of the cross section (12), particularly as some other estimates are much lower, see Section 7.4.

Exclusive diffractive processes of the type  $\bar{p}p \rightarrow \bar{p} + A + p$  have *already* been observed by CDF at the Tevatron, where  $A = \gamma\gamma$  [14] or dijet [15] or  $\chi_c$  [16]. As the sketches in Fig. 5 show,

---

<sup>3</sup>The model of Ref. [12] should contain a parameter which specifies the energy interval where the assumed approximation is valid. This has not been given.

<sup>4</sup>Note that the flat  $x$ -behaviour of NLO gluons allow the justification of the inequalities in (13) below.

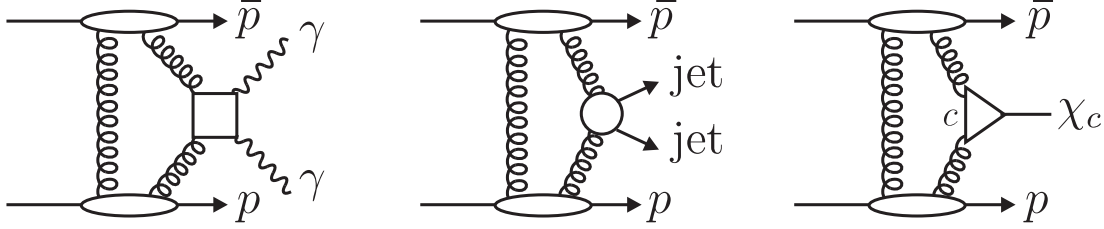


Figure 5: The mechanism for the exclusive processes observed by CDF at the Tevatron. The survival probabilities of the rapidity gaps are not indicated in the sketches.

these processes are driven by the same mechanism as that for exclusive Higgs production, but have much larger cross sections. They therefore serve as “standard candles”.

CDF observe three candidate events for  $\bar{p}p \rightarrow \bar{p} + \gamma\gamma + p$  with  $E_T^\gamma > 5$  GeV and  $|\eta^\gamma| < 1$  [14]. Two events clearly favour the  $\gamma\gamma$  hypothesis and the third is likely to be of  $\pi^0\pi^0$  origin. The predicted number of events for these experimental cuts is  $0.8^{+1.6}_{-0.5}$  [17], giving support to the ‘Durham’ approach used for the calculation of the cross sections for exclusive processes.

Especially important are the recent CDF data [15] on exclusive production of a pair of high  $E_T$  jets,  $p\bar{p} \rightarrow p + jj + \bar{p}$ . Such measurements could provide an effective  $gg^{PP}$  ‘luminosity monitor’ for the kinematical region appropriate for Higgs production. The corresponding cross

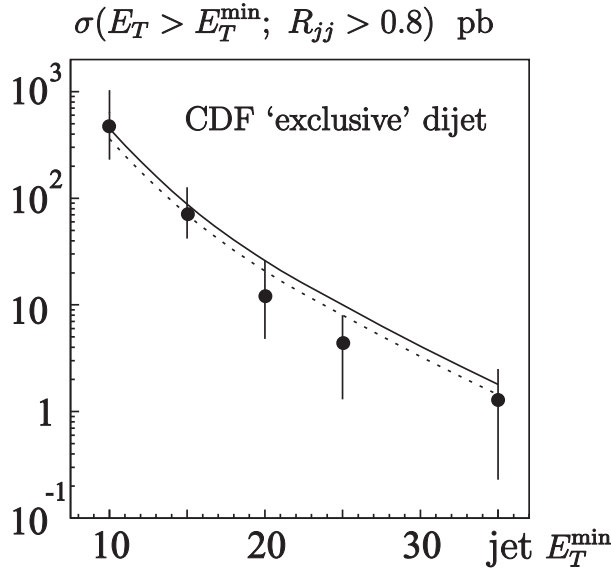


Figure 6: The cross section for ‘exclusive’ dijet production at the Tevatron as a function  $E_T^{\min}$  as measured by CDF [15]. The data integrated over the domain  $R_{jj} \equiv M_{\text{dijet}}/M_{PP} > 0.8$  and  $E_T > E_T^{\min}$ . A jet cone of  $R < 0.7$  is used. The curves are the pure exclusive cross section predicted by the ‘Durham’ model using the CDF event selection. The solid curve is obtained [3] by rescaling the parton (gluon) transverse momentum  $p_T$  to the measured jet transverse energy  $E_T$  by  $E_T = 0.8p_T$ . The dashed curve assumes  $E_T = 0.75p_T$ . The rescaling procedure effectively accounts for the hadronization and radiative effects, and for jet energy losses outside the selected jet cone.

section was evaluated to be about  $10^4$  times larger than that for the exclusive production of a SM Higgs boson. Since the exclusive dijet cross section is rather large, this process appears to be an ideal ‘standard candle’. A comparison of the data with analytical predictions, obtained using the ‘Durham’ model, is given in Fig. 6. It shows the  $E_T^{\min}$  dependence for the dijet events with  $R_{jj} \equiv M_{\text{dijet}}/M_{PP} > 0.8$ , where  $M_{PP}$  is the invariant energy of the incoming Pomeron-Pomeron system. The agreement with the theoretical expectations lends credence to the predictions for the exclusive Higgs production.

Moreover, in the *early* data runs of the LHC it is possible to observe a range of diffractive processes which will illuminate the different components of the theoretical formalism. Some information is possible even without tagging the outgoing protons [18]. For example, the observation of the rapidity,  $y_A$ , dependence of the ratio of diffractive (single gap)  $A$  production to inclusive  $A$  production will probe the effect of enhanced rescattering. The object  $A$  may be an  $\Upsilon$  or a  $W$  boson or a dijet system. The ratio should avoid normalisation problems. Other informative examples are  $W$  (or  $Z$ ) + rapidity gaps events or central 3-jet production. The exclusive process  $pp \rightarrow p + \Upsilon + p$  is interesting. For low  $p_t$  of the outgoing proton, the process is mediated by photon exchange and probes directly the unintegrated gluon distribution. At larger  $p_t$ , the process is driven by odderon exchange and could be the first hint of the existence of the odderon.

## 9 Conclusions

We emphasized the value of installing near beam proton detectors to the ATLAS and CMS experiments in order to assist the study of the Higgs sector at the LHC via the exclusive process  $pp \rightarrow p + H + p$ . This is a unique chance to study the  $H \rightarrow b\bar{b}$  decay, due to the large suppression of the QCD  $b\bar{b}$  background, and to determine the spin,  $C$  and  $P$  values of the Higgs. We described how the prediction of the  $pp \rightarrow p + H + p$  cross section depends on a mixture of ‘soft’ and ‘hard’ physics. We introduced a model of ‘soft’ high-energy  $pp$  interactions, which possessed all the requirements to give a reliable estimate of the survival probability of the rapidity gaps to both eikonal and enhanced ‘soft’ rescattering effects. Finally, we noted that the rates of the exclusive processes already observed by CDF are in good agreement with the predictions of the Durham model. This lends valuable support to the exciting proposal to indeed install the proton taggers to explore the Higgs sector via exclusive production at the LHC.

## References

- [1] M.G. Albrow [CDF Collaboration], AIP Conf. Proc. **1105**, 3 (2009), arXiv:0812.0612 [hep-ex].
- [2] M.G. Albrow *et al.* [FP420 R&D Collaboration], arXiv:0806.0302 [hep-ex].
- [3] A.D. Martin, M.G. Ryskin and V.A. Khoze, arXiv:0903.2980 [hep-ph], Acta Phys. Polonica, **40**, 1841 (2009).

- [4] M.G. Ryskin, A.D. Martin, V.A. Khoze and A.G. Shuvaev, arXiv:0907.1374 [hep-ph], J. Phys. G (in press).
- [5] M.L. Good and W.D. Walker, Phys. Rev. **120**, 1857 (1960)
- [6] V.A. Abramovsky, V.N. Gribov and O.V. Kancheli, Sov. J. Nucl. Phys. **18**, 308 (1973).
- [7] E.G.S. Luna, V.A. Khoze, A.D. Martin and M.G. Ryskin, Eur. Phys. J. **C59**, 1 (2009).
- [8] M.G. Ryskin, A.D. Martin and V.A. Khoze, Eur. Phys. J. **C60**, 249 (2009).
- [9] J. Bartels, S. Bondarenko, K. Kutak and L. Motyka, Phys. Rev. **D73**, 093004 (2006).
- [10] V.A. Khoze, A.D. Martin and M.G. Ryskin, JHEP **0605**, 036 (2006).
- [11] M.G. Ryskin, A.D. Martin and V.A. Khoze, Eur. Phys. J. **C60**, 265 (2009).
- [12] E. Gotsman, E. Levin, U. Maor and J.S. Miller, Eur. Phys. J. **C57**, 689 (2008).
- [13] L. Frankfurt, C.E. Hyde, M. Strikman and C. Weiss, Phys. Rev. **D75**, 054009 (2007);  
arXiv:0710.2942 [hep-ph];  
M. Strikman and C. Weiss, arXiv:0812.1053 [hep-ph].
- [14] T. Aaltonen *et al.* [CDF Collaboration], Phys. Rev. Lett. **99**, 242002 (2007).
- [15] T. Aaltonen *et al.* [CDF Collaboration], Phys. Rev. **D77**, 052004 (2008).
- [16] T. Aaltonen *et al.* [CDF Collaboration], Phys. Rev. Lett. **102**, 242001 (2009).
- [17] V.A. Khoze, A.D. Martin, M.G. Ryskin and W.J. Stirling, Eur. Phys. J. **C38**, 475 (2005).
- [18] V.A. Khoze, A.D. Martin and M.G. Ryskin, Eur. Phys. J. **C55**, 363 (2008).